

Cancer-associated variant expression and interaction of CIZ1 with cyclin A1 in differentiating male germ cells

Erin A. Greaves^{1,*}, Nikki A. Copeland^{2,†}, Dawn Coverley² and Justin F. X. Ainscough^{1,§}

¹Leeds Institute of Genetics, Health and Therapeutics (LIGHT), University of Leeds, Leeds LS2 9JT, UK

²Biology Department, University of York, York YO10 5DD, UK

*Present address: MRC Centre for Reproductive Health, Queen's Medical Research Institute, Edinburgh EH16 4TJ, UK

†Present address: Biomedical and Life Sciences, University of Lancaster, Lancaster LA1 4YQ, UK

§Author for correspondence (medjfxa@leeds.ac.uk)

Accepted 23 January 2012

Journal of Cell Science 125, 2466–2477

© 2012. Published by The Company of Biologists Ltd

doi: 10.1242/jcs.101097

Summary

CIZ1 is a nuclear-matrix-associated DNA replication factor unique to higher eukaryotes, for which alternatively spliced isoforms have been associated with a range of disorders. *In vitro*, the CIZ1 N-terminus interacts with cyclin E and cyclin A at distinct sites, enabling functional cooperation with cyclin-A-Cdk2 to promote replication initiation. C-terminal sequences anchor CIZ1 to fixed sites on the nuclear matrix, imposing spatial constraint on cyclin-dependent kinase activity. Here we demonstrate that CIZ1 is predominantly expressed as a predicted full-length product throughout mouse development, consistent with a ubiquitous role in cell and tissue renewal. CIZ1 is expressed in proliferating stem cells of the testis, but is notably downregulated following commitment to differentiation. Significantly, CIZ1 is re-expressed at high levels in non-proliferative spermatocytes before meiotic division. Sequence analysis identifies at least seven alternatively spliced variants, including a dominant cancer-associated form and a set of novel isoforms. Furthermore, we show that in these post-replicative cells, CIZ1 interacts with germ-cell-specific cyclin A1, which has been implicated in the repair of DNA double-strand breaks. Consistent with this role, antibody depletion of CIZ1 reduces the capacity for testis extract to repair digested plasmid DNA *in vitro*. Together, the data imply post-replicative roles for CIZ1 in germ cell differentiation that might include meiotic recombination – a process intrinsic to genome stability and diversification.

Key words: Alternative splicing, Cancer, CIZ1, Cyclin A1, Development, Male germ cell

Introduction

Mammalian development is a highly regulated process that involves programmed temporal and spatial control of DNA replication with direct impact on cell proliferation and differentiation (Hiratani and Gilbert, 2009). The balance between proliferation and differentiation involves a complex programme of transcriptional networks that facilitate appropriate cell fate decisions (Doss et al., 2012; Jiang and Hui, 2008; Lefebvre et al., 2007; Wang et al., 2008). An extreme example of strict regulation is spermatogenesis – the development of the male germ line. This involves many processes exclusive to germ cells, including stem cell self-renewal, genetic recombination and meiotic reduction of DNA content. Male germ cells also exhibit unique chromatin remodelling and condensation characteristics (Eddy, 2002). Owing to the tightly regulated sequential nature of these phases, gene expression within male germ cells is frequently stage specific (Guo et al., 2004), and whereas some genes are unique to the testis, many are also expressed in somatic cells (Wolgemuth and Watrin, 1991). In such instances, germ-cell-specific functions are provided through alternative promoter usage, testis-specific regulatory mechanisms and alternative splicing (Han et al., 2001).

Maintenance of the correct balance between spermatogonial stem cell self-renewal and germ cell differentiation requires precise control of the cell cycle (Yu and Wu, 2008). Although cell cycle regulation has been studied extensively in mitotic cells,

less is known about regulation during meiosis. It is, however, becoming increasingly clear that cyclins play an important role in this process, with some that are unique to, and others that exhibit distinct patterns of expression in, male germ cells (Wolgemuth, 2008). Cyclin A1, which is expressed primarily in germ cell lineages (Sweeney et al., 1996) and some regions of the brain (van der Meer et al., 2004), is essential for spermatocyte progression into the first meiotic division (Liu et al., 1998). Like cyclin A2, cyclin A1 associates with and activates Cdk2, albeit to a lesser extent (Joshi et al., 2009). The available evidence suggests that the cyclin-A1-Cdk2 complex plays a specific role in DNA double-strand break repair, a process that intrinsically involves DNA synthesis, strongly implicating the complex in meiotic recombination (Müller-Tidow et al., 2004).

We have previously shown that CIZ1 (Cdkn1A-interacting zinc finger protein 1) promotes initiation of DNA replication by functional co-operation with cyclin-A(2)-Cdk2 (Copeland et al., 2010; Coverley et al., 2005). Within the nucleus, CIZ1 forms foci that colocalise with DNA replication factories, and in early S phase, with newly synthesised DNA (Ainscough et al., 2007; Coverley et al., 2005). CIZ1 was originally isolated by virtue of its interaction with the cyclin-dependent kinase inhibitor, Cdkn1A (p21) (Mitsui et al., 1999) and has since been associated with a growing number of cell cycle proteins, including Cdk2 (den Hollander and Kumar, 2006), cyclin E and cyclin A2 (Copeland et al., 2010). The cyclin-interacting N-terminal region of CIZ1

encodes replication function, whereas the C-terminus acts to 'anchor' CIZ1 to the nuclear matrix where it might facilitate appropriate spatial and temporal organisation of DNA replication foci (Ainscough et al., 2007).

Ciz1 (*CIZ1*) is alternatively spliced and at least three identified variants in which exon 4, part of exon 6, or both regions together are omitted, are conserved between human and mouse indicating selective maintenance of variant function. Part of exon 8 is also alternatively spliced in both species, with increased complexity in humans (<http://www.ensembl.org>). *CIZ1* has been associated with a growing number of disorders that include rheumatoid arthritis (Judex et al., 2003), Alzheimer's disease (Dahmcke et al., 2008), and several cancers, including breast cancer (den Hollander et al., 2006), medulloblastoma (Warder and Keherly, 2003) and Ewing sarcoma (Rahman et al., 2007). Some of these disease states are associated with upregulation of *CIZ1*, whereas aberrant splicing regulation of exon 4 and 8 has been implicated in others.

The *CIZ1* variant that lacks exon 4 retains activity in DNA replication assays (Rahman et al., 2007) and by implication interaction with cyclin A2 (Copeland et al., 2010). However, unlike full-length *CIZ1*, it is not confined to subnuclear foci, and has been shown to have a dominant-negative influence on localisation of other isoforms (Rahman et al., 2007). This suggests that exon 4 plays a role in spatial targeting of *CIZ1* during DNA replication. Notably, this form has been associated with both medulloblastoma and Ewing sarcoma (Rahman et al., 2007; Warder and Keherly, 2003), implicating the variant in aberrant control of cell proliferation. However, expression and alternative splicing of *Ciz1* in a developmental context has not been previously investigated. It also remains to be substantiated whether the exon 4 lacking variant plays a role in normal development, or is restricted to disease states.

Here we demonstrate widespread low-level expression from the *Ciz1* locus during early development. Expression and alternative splicing are developmentally regulated, most notably in differentiating male germ cells where both increased levels and alternative splicing are tightly associated with differentiation. We also show that the cancer-associated *CIZ1* variant lacking exon 4 is prevalent in the male germ cells. Re-expression of multiple isoforms occurs during pachytene of meiosis I and overlaps with the window of cyclin A1 expression. At this stage, DNA replication and self-renewal has ceased, giving way to programmed post-replicative differentiation events, including genetic recombination, in which cyclin A1 is implicated (Müller-Tidow et al., 2004). We demonstrate that *CIZ1* and cyclin A1 interact directly, and that depletion of *CIZ1* from adult testis extract reduces capacity for the extract to mediate double-strand DNA break repair, implicating *CIZ1* in the post-replicative processes that contribute to male germ cell differentiation and genome diversification.

Results

Developmental regulation of *Ciz1* expression

Over the past decade, investigations into *CIZ1* have implied a significant role in a number of cancers (den Hollander et al., 2006; Rahman et al., 2007; Warder and Keherly, 2003) potentially through direct impact on the regulation of DNA replication (Coverley et al., 2005; den Hollander and Kumar, 2006). To date, most of the analyses have been performed using actively proliferating mammalian cell cultures, whereas little has

been done to explore its role *in vivo*, where cells are under developmentally specified spatial and temporal regulation. We therefore carried out a systematic investigation to profile expression and localisation of *Ciz1* during embryonic and post-natal development of the mouse using a quantitative PCR (qPCR) approach (Fig. 1).

Previous work and bioinformatics analysis indicated that *Ciz1* (*CIZ1*) is subject to a high degree of alternative splicing around the N-terminal replication domain, particularly between exons 2 and 8 (Fig. 1A and below). We used a primer probe set that amplifies outside of this region (exons 10–11) to detect the majority of *Ciz1* isoforms. When applied to a tissue array containing 36 individual samples, plus a range of additional samples generated in triplicate (Fig. 1B; supplementary material Tables S1, S2), we found that *Ciz1* levels were highly variable, but detectable in most samples. Low levels were detected at all embryonic stages examined (E7–E17) with notable downregulation at or shortly after birth. In day 1 neonates, *Ciz1* expression was almost undetectable in all tissues tested, however by day 21, expression in the testis was upregulated more than 100-fold relative to neonatal testis (supplementary material Table S1). Expression in testis continues to increase such that by day 84 (adult) levels are up to 300-fold higher than in neonatal testis. An increase was also observed in most other adult tissues to levels comparable with those in the embryo, with the notable exception of skin and skeletal muscle, where levels remained over 1000-times lower than adult testis (Fig. 1B; supplementary material Table S2).

CIZ1 is reported to be a hormonally responsive gene, with significantly increased levels in oestrogen-responsive breast cancer cells, and also in response to glucocorticoid receptor activation (den Hollander et al., 2006; Hakim et al., 2009). We therefore examined *Ciz1* levels in breast tissue at different stages of pregnancy, lactation and involution (Fig. 1B). No evidence of altered expression was observed, in comparison to breast tissue from non-pregnant females, suggesting that (mouse) *Ciz1* does not respond directly to oestrogen *in vivo* under normal developmental cues.

Northern blot analysis supported the qPCR results, providing a direct measure of *Ciz1* transcript level without amplification, and an indication of the size of predominant mRNA species. A radio-labelled probe against the 3' region of the gene (Fig. 1A) was hybridised to embryonic stage and adult tissue-specific RNA blots (Fig. 1C). The major mRNA species was detected at approximately 2.8 kb and, when adjusted for levels of the β -actin gene, appeared relatively constant through all stages of embryonic development (E5–E19). As development approached term, an additional truncated transcript (~1 kb) was also evident, which was not observed at any other stage or in adult tissues. This transcript, which might indicate a switch towards expression of alternatively spliced, truncated or antisense transcripts, has not been investigated further here.

Analysis of adult tissues was consistent with the qPCR data, showing increased tissue-specific divergence with notable high-level expression in testis and low-level expression in skeletal muscle. Northern blot analysis using total RNA from key stages of testis development confirmed that *Ciz1* expression increases in the testis after birth and is at highest levels in the adult where all stages of spermatogenesis are represented.

To investigate the cellular and sub-cellular distribution of *CIZ1* protein, we applied anti-*CIZ1* antibody 1793, which was

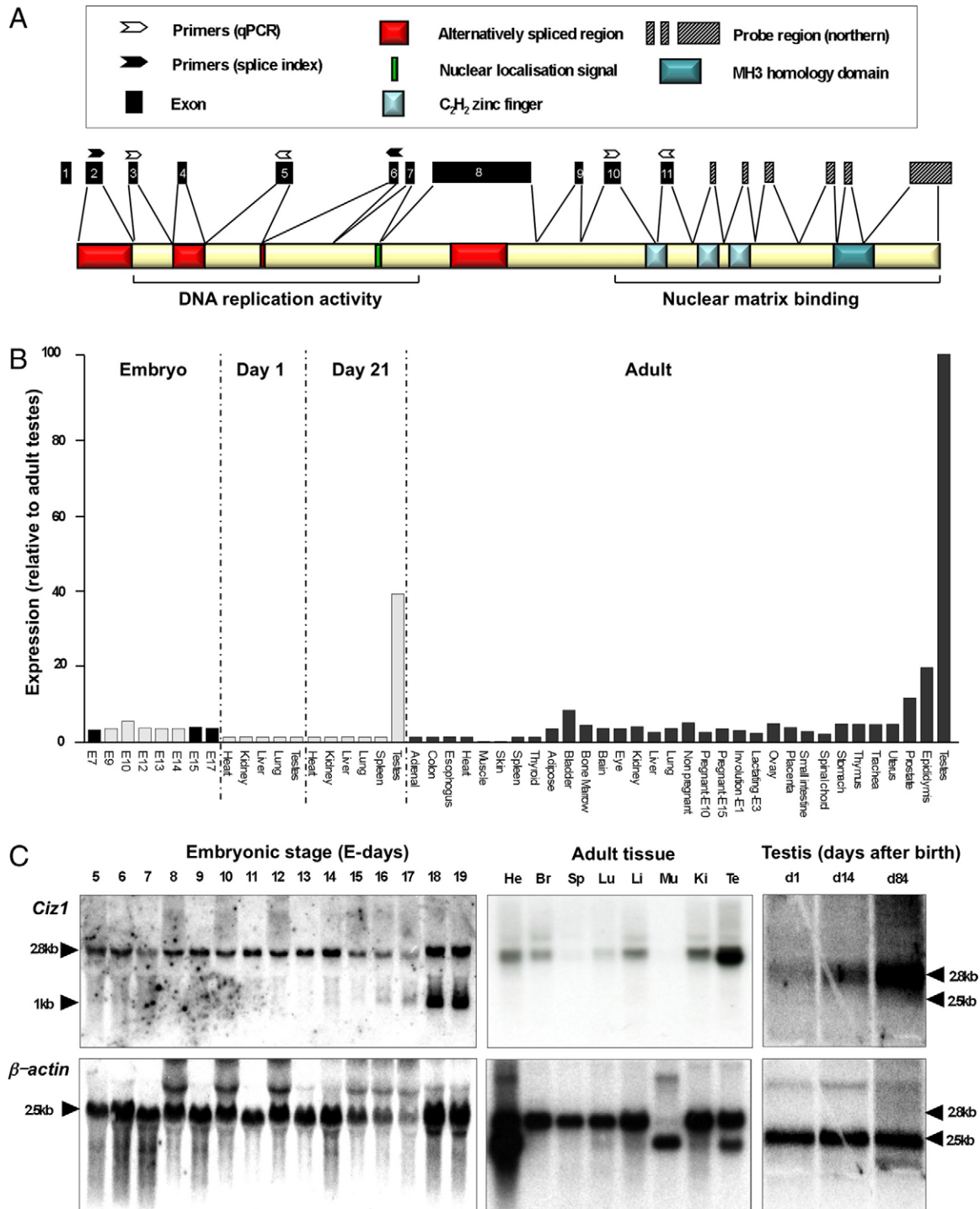


Fig. 1. Expression profile of *Ciz1*. (A) Schematic representation of *Ciz1* exon organisation and encoded protein sequence, with characterised domains (not to scale), and location of primers and northern probe used in this study. Primers for quantitative analysis (qPCR) either flanked exon 4, for use with a Taqman probe spanning the exon 3-exon 5 junction, enabling specific detection of the $\Delta e4$ variant, or amplified a non-variable internal region of the gene (exon 10–11 with internal Taqman probe) to detect total transcript levels. Primers for *Ciz1* splice index analysis (black arrows) spanned exon 2 to exon 6 and encompass a range of known alternatively spliced regions. The northern probe was directed against C-terminal sequences. (B) qPCR analysis of *Ciz1* expression in mouse tissues using the exon 10–11 primer probe set. Samples were derived from embryos or extracted from pups at day 1 and day 21 (grey bars, $n=3$ for each tissue). Adult tissues and additional embryonic samples (black bars, pooled samples) were derived from mice as represented in Origene mouse tissue qPCR array (MNRT101). All samples were normalised to *Gapdh* or *Actb*, and results expressed relative to the highest expressing sample (adult testis). Individual data points are presented in supplementary material Tables S1 and S2. *Ciz1* expression is dramatically elevated in adult testis compared with other tissues and developmental stages. (C) Northern blot analysis using the *Ciz1* C-terminal probe (top panels) followed by rehybridisation with *Actb* (bottom panels) to control for RNA loading. *Ciz1* expression is detected at all stages of embryogenesis and in a range of adult tissues. Significant upregulation is detected during testis maturation. He, heart; Br, brain; Sp, spleen; Lu, lung; Li, liver; Mu, skeletal muscle; Ki, kidney; Te, testis.

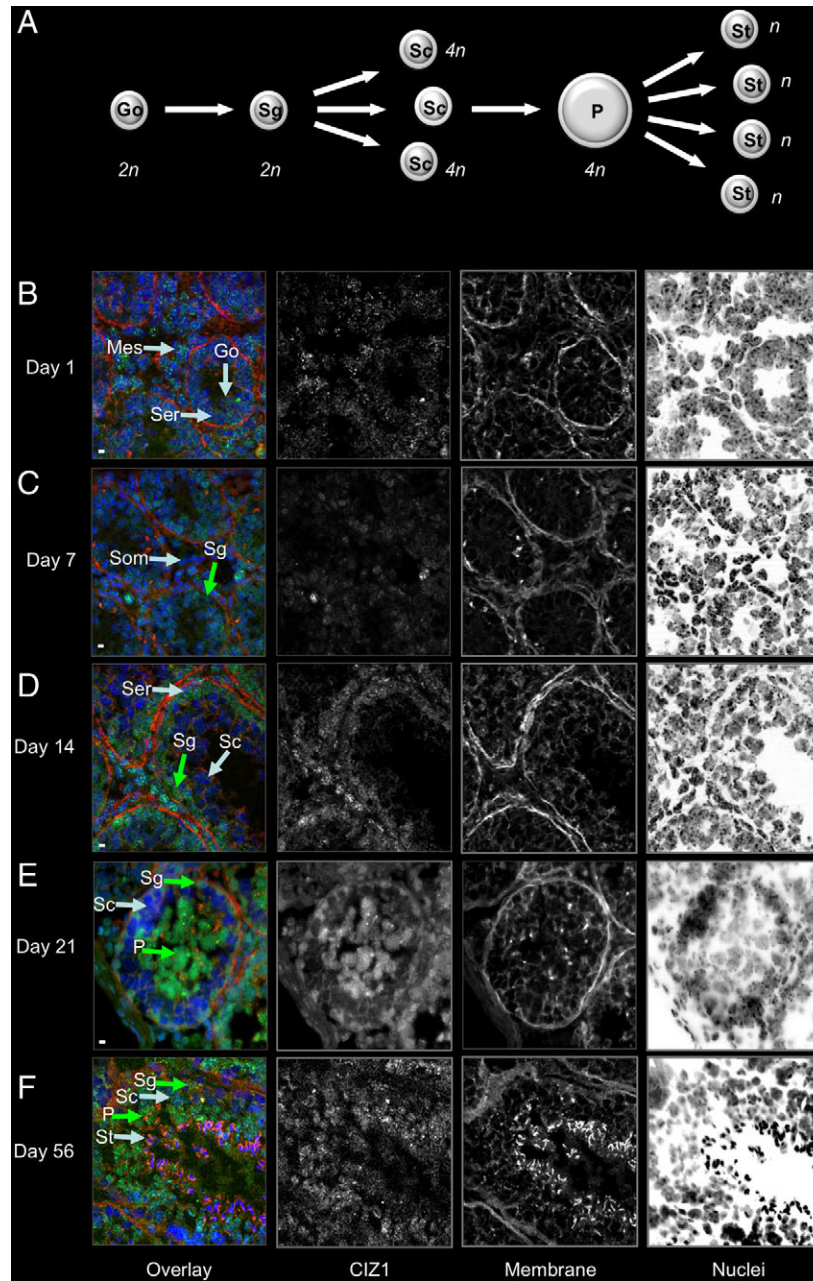


Fig. 2. CIZ1 protein localisation during male germ cell differentiation. (A) Schematic representation of spermatogenesis. Quiescent diploid ($2n$) gonocytes (Go) re-enter the cell cycle after birth and become mitotically active spermatogonia (Sg), which in addition to self-renewing, give rise to mitotically inactive spermatocytes (Sc) with a duplicated genome ($4n$). These progress through meiosis, with the pachytene (P) stage extended over 8.5 days in the mouse. Meiotic divisions give rise to four haploid (n) condensing spermatids (St) from each spermatocyte. (B–F) Images of seminiferous tubules from the testes of mice at the indicated number of days after birth. DNA is counterstained with Hoechst 33258 (Nuclei, right panels) and the images inverted to show degree of nuclear condensation. In the overlay column (left panels) nuclei are shown in blue. Membranes are stained with Rhodamine-labelled wheat germ agglutinin (shown in red in the overlay), and CIZ1 is detected with anti-CIZ1 antibody 1793 (green in the overlay). Green arrows indicate CIZ1-positive germ cells. Grey arrows indicate CIZ1-negative germ cells and somatic cells. Scale bars: 10 μ m. Go, gonocyte; Mes, mesenchymal cell; P, pachytene spermatocyte; Sc, pre-pachytene spermatocyte; Ser, sertoli cell; Sg, spermatogonia; Som, somatic cell; St, spermatid. (B) At day 1, CIZ1 protein is minimal in the gonocytes, which are located centrally in the seminiferous tubule and are non-proliferative. Quiescent Sertoli cells lining the basal membrane of the tubule are also negative. CIZ1 is more readily detected in the proliferating mesenchymal cells of the interstitial space, which account for approximately 50% of cells in this compartment (Vergouwen et al., 1991). (C) At day 7, immunoreactivity is low in spermatogonia and the majority of somatic cells. (D) At day 14 a band of CIZ1-expressing cells is seen lining the tubule basal membrane, consisting of both mitotically active spermatogonia and Sertoli cells. By contrast, cells located more centrally in the tubule do not express CIZ1 protein. At this stage and location, the most differentiated cell types present are early primary spermatocytes (pre-leptotene/zygotene) that are derived directly from the spermatogonia, and are committed to the process of meiotic reduction. (E) At day 21, two qualitatively distinct subpopulations of CIZ1-expressing cells are found within the tubule: (1) a small number of basal membrane associated cells consistent with mitotically active spermatogonia and (2) centrally located pachytene spermatocytes. A band of non-expressing pre-pachytene spermatocytes is also evident separating the two subpopulations. (F) At day 56 (adult), the complete process of spermatogenesis is represented. Two zones of CIZ1 expressing cells are again evident, plus two zones of non-expressing cells. The non-expressing zones are (1) early post-mitotic spermatocytes, and (2) differentiated and compacted spermatids and spermatozoa.

raised against an N-terminal fragment of murine CIZ1 (Ainscough et al., 2007; Coverley et al., 2005; den Hollander et al., 2006), to cryosections from a range of tissues (supplementary material Fig. S1). CIZ1 was readily detectable in the nucleus of most cells of E12 and later stage embryos (supplementary material Fig. S1A; data not shown), but showed greater restriction in adult tissues that correlated with the observed mRNA levels. Notably, in adult heart, CIZ1 protein was evident in cardiomyocytes but not in cardiac fibroblasts (supplementary material Fig. S1B). Consistent with expression at the mRNA level, CIZ1 protein was barely detectable in adult lung, muscle or ovary (supplementary material Fig. S1C–E).

Together, the data show that *Ciz1* is (1) expressed at low levels during embryogenesis, including key stages of organogenesis and foetal growth, (2) downregulated in neonatal tissues, and (3) progressively upregulated in testis after birth. These findings led us to investigate the behaviour of *Ciz1* in the male germ line.

Dynamic regulation of CIZ1 protein during male germ cell differentiation

Germ cell differentiation is a continual process that is spatially compartmentalised within the tubules of the mature testis (schematically represented in Fig. 2A). In brief, undifferentiated germ cells are located at the basement membrane giving rise to mature spermatozoa that are located and shed from the centre of the tubule. As spermatogenesis progresses, quiescent undifferentiated germ cells (gonocytes, Go) of the neonate become undifferentiated spermatogonia (Sg) that continue to proliferate resulting in production of large numbers of differentiating spermatocytes (Sc). Each primary spermatocyte undergoes a lengthy pre-meiotic phase in which the pachytene (P) stage is extended for a period exceeding one week. This is followed by the first and second meiotic divisions, giving rise to four haploid spermatids (St) per spermatocyte. In the adult mouse testis, the complete process is continuously progressing in waves that are characterised into 12 definable stages, with transit from stage 1–12 taking 8.5 days (Russell et al., 1990). Thus at any one position within the tubule, only a subset of differentiation stages can be observed, with the same differentiation profile being reproduced at that location every 8.5 days. The tightly regulated temporal and spatial organisation of spermatogenesis readily enables identification of stage-specific differentiation using histological techniques. To analyse distribution of CIZ1 protein within the testis anti-CIZ1 antibody 1793 was applied to cryosections of testes from a range of developmental stages (Fig. 2B–F).

In the immature testis, CIZ1 immunoreactivity was low in all cell types (Fig. 2B,C). However, by day 14, a distinct band of CIZ1-positive cells was observed lining the basement membrane of the tubules, consistent with both mitotically active spermatogonia (Sg) and sertoli (Ser) cells (Fig. 2D). At day 21, an additional distinct sub-population of CIZ1-expressing cells was observed centrally within the tubule (Fig. 2E), with a reduced proportion of basal-membrane-associated cells remaining positive for CIZ1. Often the basal cells were seen in pairs, reminiscent of proliferative A paired spermatogonia connected by intercellular bridges (Russell et al., 1990). Other cell types in this location are differentiating spermatogonia (Sg) and sertoli (Ser) cells, both of which are no longer proliferative (Vergouwen et al., 1991). Thus, undifferentiated spermatogonia are the only proliferative cells remaining within the tubule. The second CIZ1-positive sub-population also exhibit significant nuclear expansion, consistent with the pachytene (P) stage. Notably, pre-pachytene spermatocytes located between the two positive sub-populations showed no CIZ1 immunoreactivity.

Observation of numerous adult stage tubule cross-sections demonstrated (1) low-level CIZ1 immunoreactivity in mitotically active spermatogonia (Sg) at the basement membrane; (2) a band of non-expressing cells consistent with early post-mitotic spermatocytes (Sc); (3) a band of highly expressing cells consistent with pachytene spermatocytes (P) and post meiotic round spermatids; and (4) a central band of non-expressing, more differentiated and compacted spermatids (St) and spermatozoa (Fig. 2F). In summary, the expression analysis indicates that old CIZ1 is ‘depleted’ from mitotically active germ cells as they differentiate into non-replicative spermatocytes. ‘Replacement’ CIZ1 is generated later in the differentiation process during pachytene of meiosis I. The results suggest that newly formed CIZ1 plays a role in nuclear function above and beyond its defined role in DNA replication.

Developmental regulation of *Ciz1* alternative splicing

Bioinformatic and experimental investigations have identified a number of regions of *Ciz1* that are subject to alternative splicing. We previously reported a mouse embryonic variant, termed *ECiz1*, that lacks regions of exons 2, 6 and 8 (Ainscough et al., 2007; Coverley et al., 2005). Human isoforms lacking exon 4 have been reported in tumour cell lines (Rahman et al., 2007), and in combination with a 15 bp region of exon 6 in medulloblastoma (Warder and Keherly, 2003). For most of the known alternative splicing events, the boundaries are identical in human *CIZ1* and

Table 1. Primers and product sizes for non-quantitative RT-PCR analyses

Gene	Forward primer	Reverse primer	Product size (bp)
<i>Ciz1</i>	CAGTCCCCACCACAGGCC	GGCTTCCTCAGACCCCTCTG	FL: 525 Δe6a: 510 Δe4: 453 Δe4,6a: 438 Δe3: 408 Δe3,6a: 393 Δe3,4: 336 Δe3,4,6a: 321
<i>Stra8</i>	GTTTCCTGCGTGTTCACAAG	CACCCGAGGCTCAAGCTTC	151
<i>Syp3</i>	ATGCTTCGAGGGTGTGGG	TTCCACCAGGCACCATCTTT	76
<i>Act</i>	GTGTGCAGCCTGCACAA	ACTGGCGGTCTTGAAAGCA	71
<i>Actb</i>	CTTTGTGTAAGGTAAGGTGTGCAC	CATTGGCATGGCTTTGTTT	601

Anticipated product sizes for *Ciz1* take account of putative splicing combinations observed in this study only.

mouse *Ciz1*, implying functional conservation. To assess the alternative splice forms in a developmental context, we designed primers that span the most affected region, exons 2–6 (Fig. 1A; Table 1). Relative complexity of variant expression within this region was assessed in a range of adult tissues (Fig. 3A). A single band was detected at the predicted size for full-length *Ciz1* across the region, in somatic tissues such as heart, skeletal muscle and lung, and in ovary. By contrast, multiple distinct products were detected at significant levels in adult testis. Analysis of testis from a range of postnatal stages showed that the production of specific isoforms is developmentally regulated, with primarily full-length product in neonatal testis followed by a progressive age related increase in alternative splicing (Fig. 3B). Densitometric measurement of four regions containing isoforms was used to produce a developmental ‘splice index’ for *Ciz1* (Fig. 3C), which indicated that the major transition to production of alternatively spliced forms occurs between 2–3 weeks of postnatal development. This correlates with the point at which *Ciz1* expression levels increase (Fig. 1B), and coincides with the onset of spermatogenesis, characterised by completion of meiosis in the first cohort of germ cells (Bellvé et al., 1977).

At least seven isoforms of *Ciz1* are expressed during testis development

Amplification products generated with primers spanning exons 2–6 were isolated, cloned and sequenced. In total, 20 random individual clones were analysed from day 14 (juvenile) and day 84 (adult) testis, which were compared with 20 clones from a range of other adult tissues (supplementary material Table S3). This generated an overview of variant expression that could be assessed in conjunction with the quantitatively more accurate but qualitatively less informative splice index analysis. Sequencing identified at least seven different *Ciz1* isoforms in the testis (supplementary material Table S3; Fig. 4A,B) and, consistent with visualization of RT-PCR products (Fig. 3A), far fewer in adult somatic tissues.

In the testis, alternative splicing excludes exons 3, 4 and the first five amino acids (DSSSQ) of exon 6 from some transcripts (Fig. 4B). Significantly, of the 140 products analysed, none were found to exclude exon 5. We previously demonstrated that mutation of a single putative Cdk phosphorylation site in exon 5 [T(191/2)A] has major impact on the DNA replication activity of CIZ1 in isolated nuclei (Coverley et al., 2005). The phosphorylation site is located five amino acids upstream of the alternatively spliced DSSSQ motif (hereafter referred to as $\Delta e6a$). Taken together, the data suggest that exon 5 is constitutive and of likely basic functional importance. $\Delta e6a$ has been previously reported in both human *CIZ1* and mouse *Ciz1* genes (Coverley et al., 2005; Warder and Keherly, 2003). Although its functional significance remains unknown, this variant, like the full-length form, was isolated from all tissue types, albeit with varying frequency. Unlike $\Delta e6a$, our analysis shows that alternative splicing of exon 3 ($\Delta e3$), is a developmentally regulated event. $\Delta e3$ has not been previously reported in any species, but was observed in a significant proportion of transcripts. Our analysis also found that alternative splicing of exon 4 ($\Delta e4$) is a developmentally regulated event. Notably, $\Delta e4$ has been previously linked with human disease (Rahman et al., 2007; Warder and Keherly, 2003). The different *in vivo* combinations of alternative splicing provide the potential for dramatic effects on translation (supplementary material Fig. S2), although $\Delta e4$ and

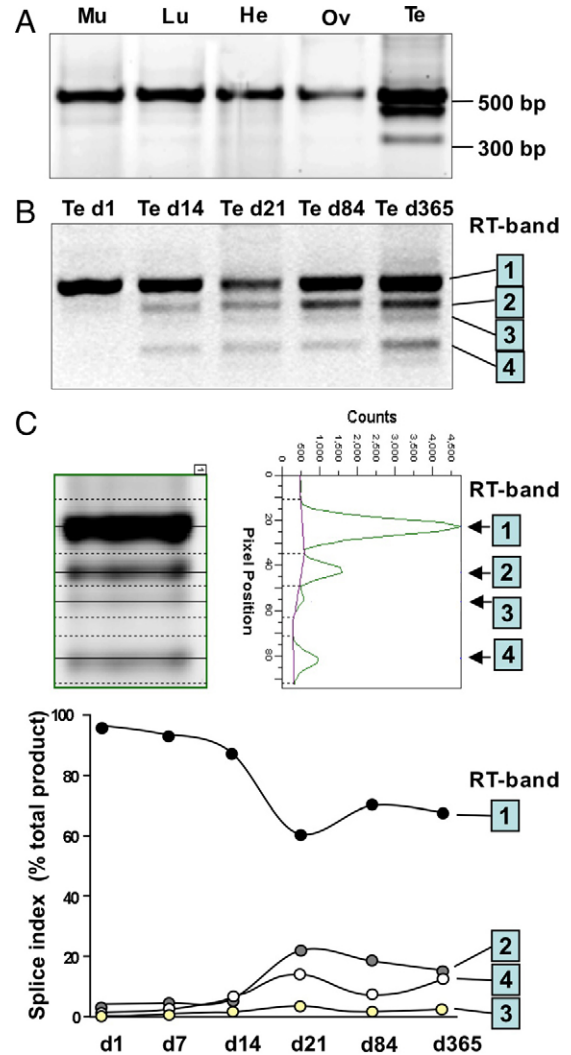


Fig. 3. *Ciz1* is alternatively spliced in testis. (A) RT-PCR analysis of adult somatic tissues, ovary and testis, using primers that amplify from exon 2 to exon 6 of *Ciz1*. The amount of product loaded was adjusted so that equivalent levels of ‘full-length’ product can be seen between lanes to enable clear comparison of the ratios of alternatively spliced products expressed in each sample. Splice index analysis indicates that, in somatic tissues and ovary, more than 95% of total product runs in the position expected for full-length transcript between exon 2 and 6, that would also include a known product lacking 15 bp of exon 6 (see below and Fig. 4). By contrast, significant alternative splicing is detected in the testis. DNA sequence analysis of the individual products identified seven different isoforms (see Fig. 4). Mu, skeletal muscle; Lu, lung; He, heart; Ov, ovary; Te, testis. (B) Developmental analysis of *Ciz1* splicing in testis reveals a progressive increase in expression of at least four clearly resolvable differentially spliced products (denoted RT, bands 1–4). Age of mice from which testis were taken is shown in days (d). (C) The relative amount of product in RT bands 1–4 in B was determined by densitometry to generate a ‘splice index’, showing a transition from 96.0, 2.2, 0.0, 1.8, respectively, in neonatal testes (d1) to 69.0, 16.0, 2.0, 13.0 in adult testes (d365).

$\Delta e6a$ cause deletion of specific sequences without altering the reading frame. Owing to the previous association of $\Delta e4$ with cancer in humans, and the evidence that CIZ1 lacking exon 4 retains DNA replication activity (Rahman et al., 2007), we examined expression of this variant in more detail using a variant

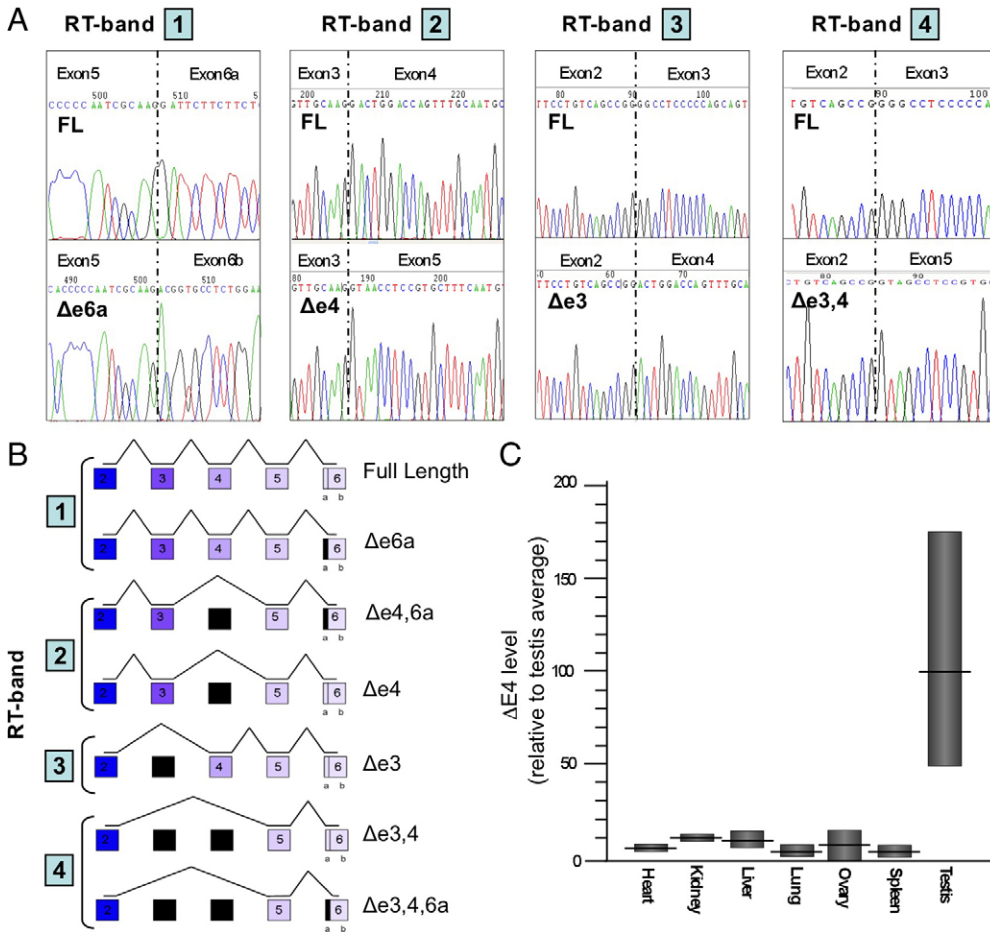


Fig. 4. *Ciz1* $\Delta e4$ is enriched in testis. (A) Representative chromatograms of alternatively spliced *Ciz1* transcripts showing sequence traces across exon junctions. Top traces show appropriate splicing for generation of full-length (FL) product. Bottom traces show different alternative splicing events. Numbers above chromatogram traces indicate band region shown in Fig. 3 from which splice forms are derived. (B) Schematic representation of all transcript forms observed in testis, derived from cloning and sequencing of individual transcripts. Frequency of individual splicing events is shown in supplementary material Table S3. Individual exons are numbered. Alternatively spliced regions are shown in black. No evidence was found for alternative splicing of exon 5. (C) qPCR analysis using the $\Delta e4$ variant specific exon 3–5 primer probe set (Methods). Expression is shown relative to testis, which was given an arbitrary average value of 100. The range in expression levels, depicted by grey bars, indicates a high degree of variability in expression of $\Delta e4$ between individual testes samples isolated from mice of similar age. Note that this assay does not detect products that lack exon 3 in combination with $\Delta e4$, and thus under-represents the true level of exon 4 lacking product relative to full-length product.

selective qPCR primer–probe set. The probe hybridizes to the exon 3–5 splice boundary and therefore specifically detects the $\Delta e4$ product only. As expected, the $\Delta e4$ variant was found at significantly higher levels in adult testis than any other tissue tested (Fig. 4C).

***Ciz1* expression is upregulated in post-mitotic spermatocytes**

To further investigate the spatial distribution of *Ciz1* splice variants in spermatogenesis, germ cells were fractionated from pooled adult testes and each fraction observed microscopically to assess purity. Fractions enriched for spermatocytes and spermatids were selected on the basis of cell size and the degree of nuclear condensation (Fig. 5A). RT-PCR for stage-specific markers was used to validate enrichment of the fractions (Fig. 5B). As in total adult testis (Fig. 3A), three dominant bands containing *Ciz1* isoforms were detected in both spermatocyte and spermatid populations, albeit at different levels (Fig. 5B). These correspond to full-length *Ciz1*, $\Delta e4$ and $\Delta e3,4$ variants, each either with or without $\Delta e6a$ (Fig. 4B). Thus, we found no evidence to suggest that *Ciz1* variant expression is associated with specific stages of differentiation in post-mitotic male germ cells. qPCR analysis on the same samples showed that the level of *Ciz1* expression is approximately 30-times higher in spermatocytes compared with spermatids (Fig. 5C). Expression of the stem cell marker *Oct4* confirmed that the spermatid fraction was highly enriched for differentiated cells, but indicated

that the spermatocyte fraction contained a significant proportion of undifferentiated cells (Fig. 5C). Given that *Ciz1* expression is very low in the immature testis at stages before spermatocyte differentiation (Fig. 1), we conclude that high-level expression of *Ciz1* is restricted to the differentiating spermatocyte population, after the final cycle of mitosis that is associated with stem cell self-renewal, and the cells are committed to meiotic reduction of DNA content.

CIZ1 expression during mitosis and in post-mitotic spermatocytes

As a first step towards understanding how CIZ1 is lost from mitotically active spermatogonia as they differentiate into non-replicative spermatocytes, we monitored the expression of endogenous CIZ1 in cycling mouse 3T3 cells using anti-CIZ1 antibody 1793. The documented nuclear focal organisation seen in interphase cells (Fig. 6A) is lost from condensed chromosomes, with a concomitant increase in cytoplasmic CIZ1 (Fig. 6B). Interestingly, CIZ1 in decondensed pachytene spermatocytes adopts a strand-like appearance that differs markedly from the focal appearance seen in cycling diploid cells (Fig. 6C). Because multiple isoforms of CIZ1 are expressed in the differentiating spermatocytes we considered the possibility that the antibody might not equally detect each variant. In fact, it is highly unlikely that $\Delta e3$ variants would be recognised because the putative truncated peptides that would be generated (supplementary material Fig. S2A) do not overlap with the

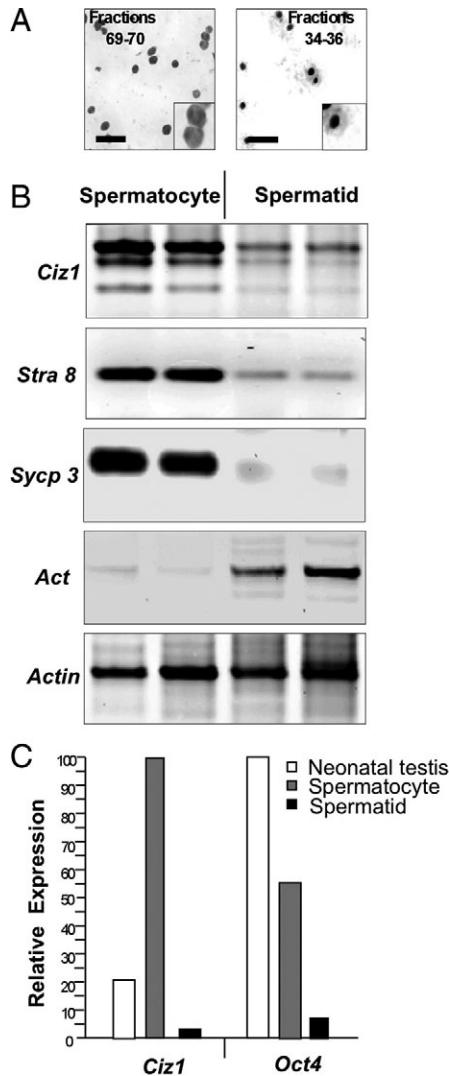


Fig. 5. Regulation of *Ciz1* splicing in spermatogenesis. (A) *Ciz1* expression in male germ cells from fractionated testes of 3-month-old mice. Fractions 69–70 are enriched for spermatocytes (left) and fractions 34–36 for condensing spermatids with compacted nuclei (right). Scale bars: 50 μ m. Insets show higher-magnification images of selected cells, which were stained with hematoxylin to visualise degree of chromatin condensation. (B) RT-PCR across exons 2–6 demonstrates that alternatively spliced isoforms of *Ciz1* are present in both spermatocyte and spermatid fractions, but that *Ciz1* levels are elevated in spermatocytes. Selected markers specific for stages of germ cell development were used to confirm enrichment of fractions (Table 1). Stimulated by retinoic acid gene 8 (*Stra8*) is a pre-meiotic marker, synaptonemal complex protein 3 (*Sycp3*) a meiotic marker, and activator of CREM in testis (*Act*) a post-meiotic marker. β -actin is shown as a control. Analysis was performed in duplicate. (C) qPCR analysis of *Ciz1* and the pluripotency marker *Oct4* in neonatal testes, spermatocytes, and spermatids. Results are shown relative to the highest expressing sample for each gene, given an arbitrary value of 100. *Ciz1* expression in spermatocytes is approximately 30-fold that in spermatids. *Oct4* is also detected at higher levels in the spermatocyte fraction than the spermatid fraction indicating that the spermatocyte fraction contains a significant proportion of undifferentiated cells.

sequences used to generate the antibody (Coverley et al., 2005). However, $\Delta 6a$ variants should be recognised, because this sequence was also excluded from the fragment that was used to generate the antibody. We found that the antibody was equally

capable of detecting recombinant CIZ1 both with and without exon 4 (supplementary material Fig. S3A). We next examined, using GFP–CIZ1 expression clones, how readily the $\Delta 4$ variant could be displaced from chromatin. As shown previously (Ainscough et al., 2007), the full-length protein was highly resistant to extraction with 0.5 M salt. By contrast, the $\Delta 4$ variant was fully extractable, suggesting that this region modulates CIZ1 displacement from chromatin (supplementary material Fig. S3B,C). Thus, a mechanism could be invoked whereby a proportion of ‘used’ CIZ1 is released at mitosis, allowing for generation of fresh CIZ1 foci. If a mark (or memory) is retained on the nuclear matrix to direct localisation of newly synthesised CIZ1 to fixed sites then subnuclear patterning might be maintained from generation to generation facilitating self-renewal. Active removal of such a mark, leading to loss of memory, however, would facilitate widespread remodelling of CIZ1 localisation in response to coincident developmental and cell-fate-specific cues.

CIZ1 interacts with cyclin A1 in adult testes

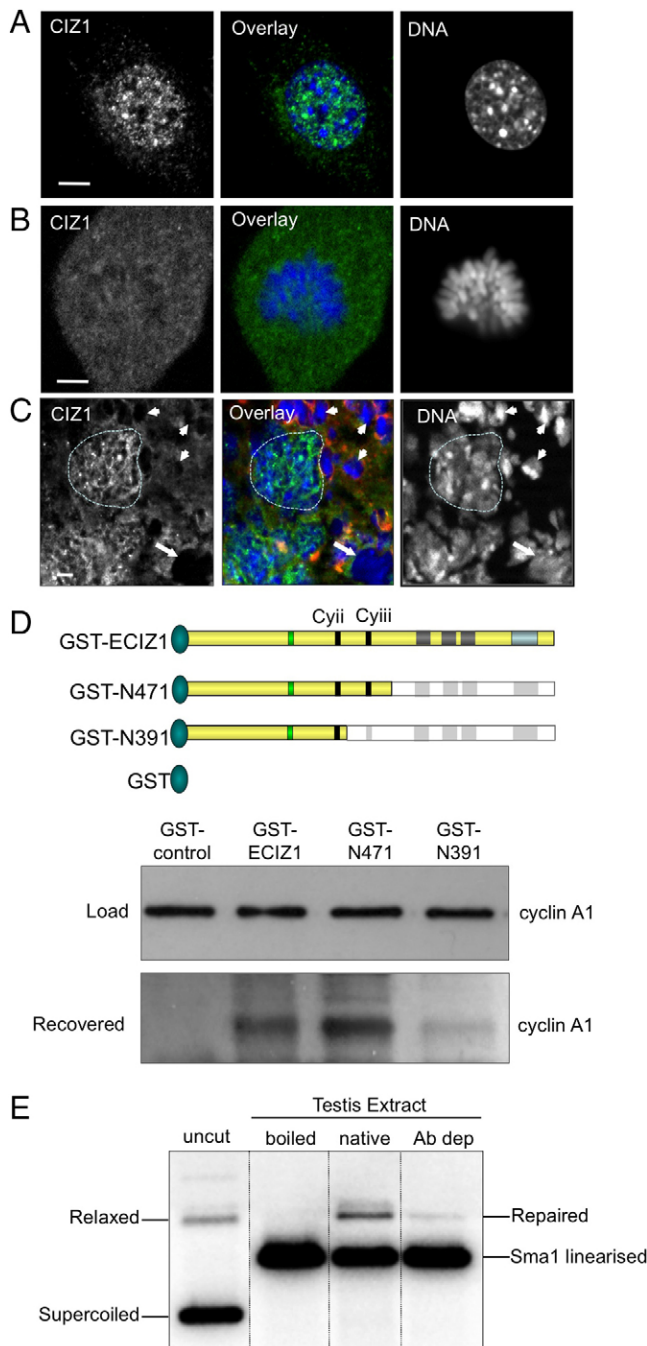
Regulated re-expression and redistribution of CIZ1 in pachytene spermatocytes closely parallels that of the germ-cell-enriched cyclin A2 homologue, cyclin A1 (Wolgemuth, 2008). As male germ cells differentiate, cyclin A2 is expressed in mitotic spermatogonia and pre-meiotic spermatocytes, then downregulated in early meiotic prophase and subsequently ‘replaced’ by cyclin A1 during pachytene (Ravnik and Wolgemuth, 1999). The close parallel between expression of CIZ1 and the A-type cyclins led us to investigate possible interaction between them. In vitro studies strongly support a role for CIZ1 in the mitotic cell cycle, through functional interaction with cell cycle regulators including Cdk2, cyclin E and cyclin A2 (Copeland et al., 2010; Coverley et al., 2005; den Hollander and Kumar, 2006). Co-immunoprecipitation experiments demonstrated interaction between CIZ1 and cyclin A1 in adult testis extract (supplementary material Fig. S3D). Using similar approaches to those used to demonstrate interaction with cyclin A2 (Copeland et al., 2010), we found that GST-tagged ECIZ1 and the derived replication active N-terminal fragment N471 (Ainscough et al., 2007; Copeland et al., 2010; Coverley et al., 2005) were able to recover cyclin A1 from lysates of 4-month-old testes. Conversely, the ECIZ1 fragment N391, which lacks the cyclin A interaction sites and the ability to function in DNA replication (Copeland et al., 2010), showed reduced affinity for cyclin A1 (Fig. 6D). Together with our previous analyses, the data demonstrate that CIZ1 interacts with both of the A-type cyclins and that the same protein domain might be involved. This implies two distinct functions: CIZ1–cyclin-A2 in DNA replication, and CIZ1–cyclin-A1 in the process of male germ cell differentiation. To begin to address a possible role for CIZ1 in male germ cell differentiation, we carried out an in vitro DNA double-strand break repair assay as described previously (Müller-Tidow et al., 2004). This showed that immunodepletion of CIZ1 significantly reduced the ability of testis extract from 4-month-old mice to rejoin linearised plasmid template (Fig. 6E). The results are consistent with a role for the CIZ1–cyclin-A1 complex in the regulation of recombination events during meiosis.

Discussion

To our knowledge, this is the first investigation of the regulation and interactions of CIZ1 during mammalian development. Our findings demonstrate that *Ciz1* is widely expressed, and

importantly provide new insight by implying an *in vivo* role for CIZ1. Together, the analyses demonstrate that a complex array of CIZ1 variants, some previously implicated in cancer, are produced in a developmentally regulated and tissue-specific manner. CIZ1 expression is maintained at low levels in cells that are actively growing and proliferating, throughout embryonic and neonatal development. However, in addition to its role in DNA replication in mitotically active cells (Coverley et al., 2005), the results suggest a role for CIZ1 and at least one of its cancer-associated variants in post-replicative male germ cell differentiation.

Appropriate control of germ cell self-renewal and differentiation, is modulated by a range of proteins that include



the cyclins. These have well-characterised roles in DNA replication and exhibit strict temporal regulation in germ cells (Yu and Wu, 2008). We have shown that the CIZ1 germ cell expression profile overlaps with that of germ-cell-enriched cyclin A1 and that the two proteins interact. Deletion of cyclin A1 results in male sterility as a result of meiotic arrest, increased germ cell apoptosis and de-synapsis abnormalities (Liu et al., 1998). Furthermore, cyclin A1 is upregulated in response to DNA damage, and in complex with Cdk2, regulates DNA double-strand break repair (Müller-Tidow et al., 2004). Significantly, this repair process is prevalent in pachytene spermatocytes and is essential to successful completion of meiotic recombination. Our recent work (including this analysis) has shown that CIZ1 interacts directly with cyclin E and cyclin A, probably providing a stable nuclear-matrix-associated scaffold directing the cyclins to appropriate subnuclear sites (Copeland et al., 2010). The data suggest that CIZ1 might also play a role in regulating meiotic progression, potentially through directing cyclin-A1-Cdk2 to double-strand breaks during meiotic recombination.

During DNA replication in somatic cells, CIZ1 tethers its binding partners to the nuclear matrix by a C-terminal anchor domain (Ainscough et al., 2007). CIZ1 also exists in subnuclear foci that appear to mark the sites at which DNA replication will take place in S phase (Ainscough et al., 2007). Unlike full-length CIZ1, the Δ e4 variant can be extracted from chromatin using 0.5 M salt and does not localise to subnuclear foci, although it does remain active in DNA replication assays. Moreover, increasing the level of CIZ1 Δ e4 hinders the full-length protein from forming foci, suggesting that expression of Δ e4 variants influence where in the nucleus DNA replication takes place (Rahman et al., 2007). *In vivo*, the Δ e4 form is observed at very low levels in terminally differentiated cell types that have in common limited proliferation and/or differentiation potential. CIZ1 Δ e4 is also barely detectable in cultured cells that are able to freely proliferate but have limited capacity to alter phenotype. Conversely, in differentiating male germ cells that have ceased the replication process, expression of CIZ1 Δ e4 increases significantly with maximal levels in the pachytene spermatocytes.

Fig. 6. CIZ1 is released during mitosis and interacts with cyclin A1 in adult testes. (A) Cycling cultured mouse 3T3 cell nucleus in interphase. CIZ1 (green) is localised to subnuclear foci. DNA (blue) is stained with Hoechst 33258. (B) CIZ1 is released into the cytoplasm upon chromosome condensation and nuclear membrane breakdown. (C) In pachytene spermatocytes (outlined) CIZ1 adopts a strand-like appearance, distinct from that seen in other cell types. CIZ1 is undetectable in condensing (arrow) and condensed (arrowheads) spermatids. Scale bars: 5 μ m. (D) GST-tagged CIZ1 isoform (ECIZ1) and derived N-terminal fragments N471 and N391 were used as bait proteins, and GST alone as a negative control. Western blot analysis shows endogenous cyclin A1, recovered (bottom) from cell lysates (top) prepared from testes of 4-month-old mice. Constructs are as depicted with functional domains as indicated in Fig. 1A. The GST tag is represented as a blue oval. As for cyclin A2 (Copeland et al., 2010), the 80 amino acid region between N391 and N471 is required for efficient interaction with cyclin A1. Position of defined cyclin binding sites Cyii and Cyiii are indicated. (E) *Sma*I-linearised plasmid migrates more slowly than supercoiled plasmid, but faster than relaxed (circular) plasmid. Native adult testis extract supports rejoining of the separated DNA ends (repaired). This activity is lost when the extract is boiled. Immunodepletion of CIZ1 results in a significant reduction in religation of the DNA double strand break. Plasmid forms were visualised by Southern blot and quantified by phosphorimager.

Table 2. Assay details for primer–probe sets used for qPCR gene expression analysis

Gene	Gene region	Assay	Product size (bp)
<i>Ciz1</i>	Exon 10–11	Mm00503766_m1	77
<i>Gapdh</i>	Exon 2–3	Mm99999915_g1	107
<i>Actb</i> (β-actin)	Exon 6	Mm00607939_s1	115
<i>Oct4</i>	Exon 2–3	Mm00658129_gH	148
<i>Stra8</i>	Exon 8–9	Mm01165142_m1	71
<i>Sycp3</i>	Exon 4–5	Mm00488519_m1	136

The mechanisms that regulate production of different splice variants are extremely complex and still far from fully understood (Chen and Manley, 2009). What is clear is that control over the relative balance of individual variants for some genes is critically important to normal cellular behaviour in mammalian development. This includes regulation of stem cell pluripotency and differentiation, as demonstrated recently for a novel stem-cell-specific isoform of FOXP1 that stimulates expression of key pluripotency genes (Gabut et al., 2011). In this respect, it is worth re-emphasising that significant CIZ1 Δe4 expression has been observed in somatic cells derived from diseased tissues (Rahman et al., 2007; Warder and Keherly, 2003), suggesting that inappropriate regulation of CIZ1 splicing might disrupt the balance between proliferation and differentiation, contributing to loss of cellular identity. We suggest that, in the post-replicative germ cells, induction of variant expression facilitates remodelling of CIZ1 on the nuclear matrix. This would enable clearing of stabilised replication marks, thus preparing the chromatin for subsequent remodelling (supplementary material Fig. S4). High-level expression of a broad range of CIZ1 splice variants might then facilitate progression through meiosis, in part through interaction with cyclin A1.

We recently demonstrated that another interacting partner of CIZ1, cyclin E, is recruited to the nuclear matrix as cells are induced to differentiate (Munkley et al., 2011). Cancer cells, however, do not exhibit similar matrix-association characteristics, suggesting that pre-replication complex assembly is inhibited from appropriate spatial restriction in these cells, with subsequent impact on cellular identity. By implication, therefore, we suggest that production of the cancer associated CIZ1 Δe4 variant might directly regulate matrix association characteristics of CIZ1 interacting partners during cellular differentiation.

In summary, the switch from mitotic stem cell to meiotic germ cell involves removal and replacement of CIZ1 (supplementary material Fig. S4). When new CIZ1 is produced in these cells, it occurs in multiple splice forms, at very high levels. A second round of CIZ1 loss after meiosis correlates with higher-order chromatin compaction in the mature sperm. Whether any residual CIZ1 remains in the sperm nucleus, marking specific retargeting sites on the nuclear matrix, remains to be investigated. It is possible that such a mark would facilitate establishment of nuclear organisation and differential replicative behaviour of the male and female pronuclei within the first few hours after fertilisation (Ferreira and Carmo-Fonseca, 1997). The findings we present here are consistent with the notion that self-renewal, which requires a stable nuclear conformation and gene expression signature to maintain a consistent phenotype, involves targeting of 'new' CIZ1 to 'predetermined' sites on the nuclear matrix. Whilst cells receive specific cues that induce differentiation

pathways, both chromatin and matrix are remodelled, providing opportunity for retargeting of new CIZ1 to regions that require alteration of transcriptional status or other aspects of chromatin management.

Materials and Methods

Animals

All experiments were performed using samples isolated from C57BL/6 mice, in accordance with UK Home Office regulations. After isolation, samples were washed in cold PBS and either used immediately for RNA isolation or histology, or snap frozen and stored at -80°C for later use.

Gene expression

RNA isolated from tissue samples using TRI Reagent (Ambion) was reverse transcribed with SuperScript III (Invitrogen) using random hexamers (Sigma). Specific products were amplified with Phusion high-fidelity DNA polymerase (Finnzymes) as follows: 98°C (10 seconds), followed by 33 cycles of 98°C (15 seconds), 65°C (30 seconds) and 72°C (40 seconds), with a final extension at 72°C (7 minutes). Gene-specific primers are detailed in Table 1. For qPCR, cDNAs generated as above were added to reactions containing TaqMan PCR master mix, gene-specific primers and probe (Applied Biosystems; Table 2) and amplified using an ABI 7500 Real Time PCR System as follows: 50°C (2 minutes), 95°C (10 minutes), followed by 50 cycles of 95°C (15 seconds) and 60°C (1 minute). For the *Ciz1* Δe4 gene expression assay, forward primer 5'-CCCATGCTGCAAA-GAGCTTT-3' and reverse primer 5'-TGTAAGGCTGGGAGCTGCTA-3' were used, with Taqman probe 5'-GCAag_gtAACCTCCGTGCTTCAATGTGA-3'. The Taqman probe used for specific detection of the *Ciz1*Δe4 variant was directed against the splicing junction between exons 3 and 5, shown as ag_gt. All qPCR results were analysed using 7500 System SDS software version 1.2.3 (Applied Biosystems). All samples were normalised against *Actb* or *Gapdh*. Samples used ($n=3$) are detailed in supplementary material Table S1. Samples on the OriGene MNRT101 real-time array (pooled samples) are detailed in supplementary material Table S2. Relative expression was calculated as $2^{-\Delta\text{CT}} \times 100$, and adjusted to the following arbitrary values: For *Ciz1*, adult testis = 100 (Fig. 1B, Fig. 4C); spermatocyte fraction = 100 (Fig. 5C). For *Oct4*, neonatal testis = 100 (Fig. 5C).

Cloning and sequencing

Ciz1 fragments amplified in RT-PCR reactions were separated by electrophoresis onto DE81 paper (Whatman), washed with TE containing 0.1 M NaCl, eluted into TE with 1 M NaCl, extracted with phenol–chloroform, precipitated with ethanol and cloned into pGEM-T-Easy vector (Promega). Cloned inserts were sequenced by adding 3–10 ng DNA to reactions containing 1.6 pmol M13 primer (5'-TGTAACACGACGGCCAGT-3'), ABI Big Dye Terminator mix and sequencing buffer (Applied Biosystems) as follows: 96°C (1 minute), followed by 24 cycles of 96°C (10 seconds), 50°C (5 seconds), 60°C (5 minutes). Sequences were analysed using an ABI Prism 3700 DNA analyzer (Applied Biosystems) and Chromas Lite (version 2.01) software, and aligned using GeneJockey and ClustalW (EMBL-EBL).

Northern blotting

For stage-specific testis analysis, total RNA (15 μg) mixed with three volumes of formaldehyde loading dye (Ambion NorthernMax kit) was incubated at 65°C for 15 minutes, then separated by electrophoresis through formaldehyde agarose and transferred onto Hybond N⁺ nitrocellulose membrane (Amersham). Embryonic stages and adult tissues were analysed using blots from AMS Laboratories and Clontech, respectively. Hybridisations were performed at 42°C in ULTRAhyb (Ambion) using [α - ^{32}P]dCTP (PerkinElmer)-labelled *Ciz1* (1 kb C-terminal) and *Actb* (500 bp) probes generated using a random primers DNA labelling system (Invitrogen). Membranes were stripped of the *Ciz1* probe before hybridisation with the *Actb* probe to determine relative loading. Washed blots were exposed to storage phosphor screens and analysed using a Typhoon 9410 variable mode imager (Amersham) and ImageQuantTL densitometry software.

Protein interaction

Testes were dissected from 4-month-old mice, washed in cold PBS, snap frozen, macerated and resuspended in 10× w/v of hypotonic buffer (10 mM HEPES, pH 7.8, 0.5 mM MgCl₂, 5 mM potassium acetate, 1 mM DTT, 2× complete protease inhibitor, 1 mM PMSF). Following homogenisation, insoluble material was removed by centrifugation at 13,000 r.p.m. Soluble extracts were snap-frozen and stored at -80°C. Salt extraction from insoluble material was performed in hypotonic buffer with 450 mM NaCl and 0.5% v/v Triton X-100. Testis salt extracts were diluted 1 in 4 into binding buffer [50 mM HEPES, pH 7.8, 20 mM MgCl₂, 10 mM CaCl₂, 0.04% NP 40, 1 mM DTT, complete EDTA-free protease inhibitors (Roche)]. 5 µl anti-Ciz1 antibody 1793 was added to reactions as indicated and incubated for 2 hours at 4°C. Protein-A/G beads (Pierce) were used to recover immune complexes. Beads were washed five times, boiled in SDS-PAGE loading buffer and visualised by western blot using protein-A/G-HRP (Pierce). GST-tagged protein pull-down experiments were performed using GST-tagged murine embryonic CIZ1 variant (ECIZ1) and ECIZ1 N terminal fragments (N471 and N391) that were overexpressed in *E. coli* BL21 (DE3)+pLysS and purified as described previously (Coverley et al., 2005). Purified recombinant protein was immobilised on Glutathione-Sepharose and incubated with homogenised 4-month-old testes soluble extract in binding buffer. Beads were washed five times in binding buffer and boiled in SDS-PAGE loading buffer. Load (5% of binding reaction) and recovered proteins were detected by western blotting using an antibody (1:1000) raised against the N-terminus of mouse cyclin A1 (Sweeney et al., 1996) and an anti-rabbit HRP-conjugated secondary antibody (Sigma, 1:5000). Signal was detected with EZ-ECL (Geneflow).

GFP-tagged expression constructs, nuclear extraction and anti-CIZ1 1793 antibody interaction

GFP-tagged ECIZ1Δe4 and full-length expression constructs were prepared and transfected into cycling mouse 3T3 cells grown on glass coverslips as described previously (Rahman et al., 2007). After 24–48 hours, the coverslips were flooded with 100 µl ice-cold cytoskeletal buffer with or without detergent and 0.5 M NaCl, then rinsed and fixed with 4% paraformaldehyde as described (Ainscough et al., 2007). DNA was stained with Hoechst 33258. Images were taken using a Zeiss Axiovert microscope fitted with AxioCam camera and Openlab software. Images were adjusted using Adobe Photoshop CS. For CIZ1 antibody characterisation protein extract from 3T3 cells (approximately 10⁵ per lane equivalent) transfected with empty GFP vector (Clontech), GFP-tagged ECIZ1Δe4 and GFP-tagged full-length ECIZ1 were separated by 8% SDS-PAGE, transferred to nitrocellulose, blocked and probed with anti-CIZ1 1793 (1:1000). Signal was detected with EZ-ECL (Geneflow).

DNA double-strand break repair assay

100 ng *Sma*I-linearised plasmid DNA containing GFP-tagged C-terminal region of *Ciz1* (EGFP-C275) was incubated in 50 µg protein extract prepared from adult testis (detailed above), supplemented with cell-free replication components as described (Copeland et al., 2010), for 3.5 hours at 25°C in a total volume of 20 µl. Testis extract was added to samples as either native, boiled, or following pre-depletion with 1793 antibody (1:20). Extract containing antibody was incubated for 40 minutes on ice before addition of 5 µl packed Protein-A/G beads (prewashed). After a further 40 minute incubation on ice, the beads were pelleted and the supernatant used in the re-ligation experiment alongside mock-treated control. Following incubation, 80 µl TE was added and the DNA extracted with phenol–chloroform. 25 µl of each sample was separated by electrophoresis through 0.8% agarose, transferred onto Hybond N⁺ nitrocellulose membrane (Amersham), and probed with radiolabelled CIZ1C275 fragment. After washing, the membrane was exposed to a storage phosphor screen and imaged using a Typhoon 9410 variable mode imager (Amersham).

Immunofluorescence

Testis cryosections (5 µm) were fixed in 4% paraformaldehyde followed by brief exposure to 0.05% Triton X-100 in PBS. Endogenous CIZ1 was detected with antibody 1793 (Coverley et al., 2005) followed by an anti-rabbit FITC-conjugated secondary (Sigma). Cell membranes and nuclei were visualised with wheat germ agglutinin (Vector Laboratories) and Hoechst 33258 (Sigma), respectively. Sections were mounted in VectorShield (Vector Laboratories). Images for Figs 2, 6 and supplementary material Fig. S1 were taken using a Zeiss AxioImager Z.1 epifluorescence microscope fitted with a 40× or 63× oil objective and AxioVision digital image processing software (Zeiss), then prepared using Adobe Photoshop CS.

Acknowledgements

We thank Mark Carrington and William Colledge (University of Cambridge, Cambridge, UK) for the anti-cyclin A1 antibody; A. Sedo, P. Warburton, J. Seddon, G. Higgins and N. Yuldasheva for

technical assistance; and T. Batten, D. Miller, I. Morris and M. Brinkworth for helpful discussion.

Funding

This work was supported by a Cardiovascular Research Institute at Leeds (CRISTAL) PhD studentship awarded to E.G. N.C. was funded by Yorkshire Cancer Research.

Supplementary material available online at

<http://jcs.biologists.org/lookup/suppl/doi:10.1242/jcs.101097/-/DC1>

References

- Ainscough, J. F., Rahman, F. A., Sercombe, H., Sedo, A., Gerlach, B. and Coverley, D. (2007). C-terminal domains deliver the DNA replication factor Ciz1 to the nuclear matrix. *J. Cell Sci.* **120**, 115–124.
- Bellvé, A. R., Cavicchia, J. C., Millette, C. F., O'Brien, D. A., Bhatnagar, Y. M. and Dym, M. (1977). Spermatogenic cells of the prepubertal mouse. Isolation and morphological characterization. *J. Cell Biol.* **74**, 68–85.
- Chen, M. and Manley, J. L. (2009). Mechanisms of alternative splicing regulation: insights from molecular and genomics approaches. *Nat. Rev. Mol. Cell Biol.* **10**, 741–754.
- Copeland, N. A., Sercombe, H. E., Ainscough, J. F. and Coverley, D. (2010). Ciz1 cooperates with cyclin-A-CDK2 to activate mammalian DNA replication in vitro. *J. Cell Sci.* **123**, 1108–1115.
- Coverley, D., Marr, J. and Ainscough, J. (2005). Ciz1 promotes mammalian DNA replication. *J. Cell Sci.* **118**, 101–112.
- Dahmcke, C. M., Büchmann-Møller, S., Jensen, N. A. and Mitchelmore, C. (2008). Altered splicing in exon 8 of the DNA replication factor CIZ1 affects subnuclear distribution and is associated with Alzheimer's disease. *Mol. Cell. Neurosci.* **38**, 589–594.
- den Hollander, P. and Kumar, R. (2006). Dynein light chain 1 contributes to cell cycle progression by increasing cyclin-dependent kinase 2 activity in estrogen-stimulated cells. *Cancer Res.* **66**, 5941–5949.
- den Hollander, P., Rayala, S. K., Coverley, D. and Kumar, R. (2006). Ciz1, a Novel DNA-binding coactivator of the estrogen receptor alpha, confers hypersensitivity to estrogen action. *Cancer Res.* **66**, 11021–11029.
- Doss, M. X., Gaspar, J. A., Winkler, J., Hescheler, J., Schulz, H. and Sachinidis, A. (2012). Specific gene signatures and pathways in mesodermal cells and their derivatives Derived from embryonic stem cells. *Stem Cell Rev.* **8**, 43–54.
- Eddy, E. M. (2002). Male germ cell gene expression. *Recent Prog. Horm. Res.* **57**, 103–128.
- Ferreira, J. and Carmo-Fonseca, M. (1997). Genome replication in early mouse embryos follows a defined temporal and spatial order. *J. Cell Sci.* **110**, 889–897.
- Gabut, M., Samavarchi-Tehrani, P., Wang, X., Slobodeniuc, V., O'Hanlon, D., Sung, H. K., Alvarez, M., Talukder, S., Pan, Q., Mazzoni, E. O. et al. (2011). An alternative splicing switch regulates embryonic stem cell pluripotency and reprogramming. *Cell* **147**, 132–146.
- Guo, R., Yu, Z., Guan, J., Ge, Y., Ma, J., Li, S., Wang, S., Xue, S. and Han, D. (2004). Stage-specific and tissue-specific expression characteristics of differentially expressed genes during mouse spermatogenesis. *Mol. Reprod. Dev.* **67**, 264–272.
- Hakim, O., John, S., Ling, J. Q., Biddie, S. C., Hoffman, A. R. and Hager, G. L. (2009). Glucocorticoid receptor activation of the Ciz1-Lcn2 locus by long range interactions. *J. Biol. Chem.* **284**, 6048–6052.
- Han, S. Y., Zhou, L., Upadhyaya, A., Lee, S. H., Parker, K. L. and DeJong, J. (2001). TFIIIAalpha/beta-like factor is encoded by a germ cell-specific gene whose expression is up-regulated with other general transcription factors during spermatogenesis in the mouse. *Biol. Reprod.* **64**, 507–517.
- Hiratani, I. and Gilbert, D. M. (2009). Replication timing as an epigenetic mark. *Epigenetics* **4**, 93–97.
- Jiang, J. and Hui, C. C. (2008). Hedgehog signaling in development and cancer. *Dev. Cell* **15**, 801–812.
- Joshi, A. R., Jobanputra, V., Lele, K. M. and Wolgemuth, D. J. (2009). Distinct properties of cyclin-dependent kinase complexes containing cyclin A1 and cyclin A2. *Biochem. Biophys. Res. Commun.* **378**, 595–599.
- Judex, M., Neumann, E., Lechner, S., Dietmaier, W., Ballhorn, W., Grifka, J., Gay, S., Schölmerich, J., Kullmann, F. and Müller-Ladner, U. (2003). Laser-mediated microdissection facilitates analysis of area-specific gene expression in rheumatoid synovium. *Arthritis Rheum.* **48**, 97–102.
- Lefebvre, V., Dumitriu, B., Penzo-Méndez, A., Han, Y. and Pallavi, B. (2007). Control of cell fate and differentiation by Sry-related high-mobility-group box (Sox) transcription factors. *Int. J. Biochem. Cell Biol.* **39**, 2195–2214.
- Liu, D., Matzuk, M. M., Sung, W. K., Guo, Q., Wang, P. and Wolgemuth, D. J. (1998). Cyclin A1 is required for meiosis in the male mouse. *Nat. Genet.* **20**, 377–380.
- Mitsui, K., Matsumoto, A., Ohtsuka, S., Ohtsubo, M. and Yoshimura, A. (1999). Cloning and characterization of a novel p21(Cip1/Waf1)-interacting zinc finger protein, ciz1. *Biochem. Biophys. Res. Commun.* **264**, 457–464.
- Müller-Tidow, C., Ji, P., Diederichs, S., Potratz, J., Bäumer, N., Köhler, G., Cauvet, T., Choudary, C., van der Meer, T., Chan, W. Y. et al. (2004). The cyclin A1-CDK2 complex regulates DNA double-strand break repair. *Mol. Cell. Biol.* **24**, 8917–8928.

- Munkley, J., Copeland, N. A., Moignard, V., Knight, J. R., Greaves, E., Ramsbottom, S. A., Pownall, M. E., Southgate, J., Ainscough, J. F. and Coverley, D.** (2011). Cyclin E is recruited to the nuclear matrix during differentiation, but is not recruited in cancer cells. *Nucleic Acids Res.* **39**, 2671-2677.
- Rahman, F. A., Ainscough, J. F., Copeland, N. and Coverley, D.** (2007). Cancer-associated missplicing of exon 4 influences the subnuclear distribution of the DNA replication factor CIZ1. *Hum. Mutat.* **28**, 993-1004.
- Ravnik, S. E. and Wolgemuth, D. J.** (1999). Regulation of meiosis during mammalian spermatogenesis: the A-type cyclins and their associated cyclin-dependent kinases are differentially expressed in the germ-cell lineage. *Dev. Biol.* **207**, 408-418.
- Russell, L. D., Ettl, R. A., Sinha Hikim, A. P. and Clegg, E. D.** (1990). *Histological And Histopathological Evaluation Of The Testis*. Clearwater, FL, USA: Cache River Press.
- Sweeney, C., Murphy, M., Kubelka, M., Ravnik, S. E., Hawkins, C. F., Wolgemuth, D. J. and Carrington, M.** (1996). A distinct cyclin A is expressed in germ cells in the mouse. *Development* **122**, 53-64.
- van der Meer, T., Chan, W. Y., Palazon, L. S., Nieduszynski, C., Murphy, M., Sobczak-Thépot, J., Carrington, M. and Colledge, W. H.** (2004). Cyclin A1 protein shows haplo-insufficiency for normal fertility in male mice. *Reproduction* **127**, 503-511.
- Vergouwen, R. P., Jacobs, S. G., Huiskamp, R., Davids, J. A. and de Rooij, D. G.** (1991). Proliferative activity of gonocytes, Sertoli cells and interstitial cells during testicular development in mice. *J. Reprod. Fertil.* **93**, 233-243.
- Wang, Q., Fang, W. H., Krupinski, J., Kumar, S., Slevin, M. and Kumar, P.** (2008). Pax genes in embryogenesis and oncogenesis. *J. Cell. Mol. Med.* **12**, 2281-2294.
- Warder, D. E. and Keherly, M. J.** (2003). Ciz1, Cip1 interacting zinc finger protein 1 binds the consensus DNA sequence ARYSR(0-2)YYAC. *J. Biomed. Sci.* **10**, 406-417.
- Wolgemuth, D. J.** (2008). Function of cyclins in regulating the mitotic and meiotic cell cycles in male germ cells. *Cell Cycle* **7**, 3509-3513.
- Wolgemuth, D. J. and Watrin, F.** (1991). List of cloned mouse genes with unique expression patterns during spermatogenesis. *Mamm. Genome* **1**, 283-288.
- Yu, Q. and Wu, J.** (2008). Involvement of cyclins in mammalian spermatogenesis. *Mol. Cell. Biochem.* **315**, 17-24.